J. Opt. B: Quantum Semiclass. Opt. **1** (1999) 496–504. Printed in the UK PII: S1464-4266(99)01994-1

Quantum state transfer between motion and light

A S Parkins† and H J Kimble‡

† Department of Physics, University of Auckland, Auckland, New Zealand
‡ Norman Bridge Laboratory of Physics 12-33, California Institute of Technology, Pasadena, CA 91125, USA

Received 19 February 1999

Abstract. We describe schemes for transferring quantum states between light fields and the motion of a trapped atom. Coupling between the motion and the light is achieved via Raman transitions driven by a laser field and the quantized field of a high-finesse microscopic cavity mode. By cascading two such systems and tailoring laser field pulses, we show that it is possible to transfer an arbitrary motional state of one atom to a second atom at a spatially distant site.

Keywords: Quantum communication, cavity QED, quantized motion, nonclassical states

1. Introduction

The quantized motional states of atoms or ions in confining potentials offer interesting possibilities for a variety of applications, such as the preparation and study of nonclassical (i.e. manifestly quantum) states [1–5], and the storage and manipulation of quantum information (e.g. 'qubits'), with particular reference to quantum logic operations and quantum computing [6–12]. These possibilities stem from the relatively long coherence times that can be achieved with motional states (due to the absence of strong damping mechanisms) and the precision with which transformations between motional states can be controlled using laser-light-induced transitions.

However, while motional states are well suited to the storage and manipulation of quantum states, for the communication of quantum information from one physical location to another it is clear that photons are the preferred carriers of the information. For this reason, it is necessary to provide and examine configurations in which motional states can be efficiently and reliably transferred to states of light, and vice versa. Here enters the field of cavity quantum electrodynamics (cavity QED); in particular, configurations in which a single mode of the electromagnetic field supported by an optical cavity is strongly coupled to a transition in a single atom. It is possible, via the internal atomic transition, to also couple the cavity field to the external (quantized) motion of the trapped atom or ion [13–15], and in this paper we examine such a coupling that enables the above-mentioned state transfer.

2. Model

Our model consists of a single two-level atom (or ion) confined in a harmonic trap located inside an optical cavity.

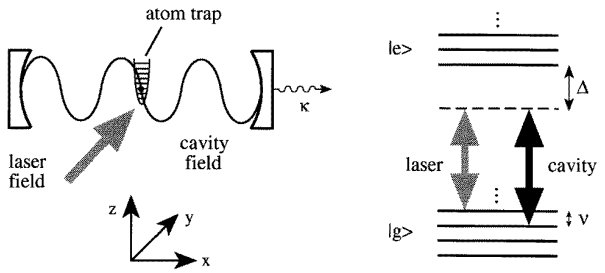

Figure 1. Schematic of experimental set-up and excitation scheme for state transfer between the motion of a trapped atom/ion and a quantized cavity mode of the electromagnetic field.

The atomic transition of frequency ω_a is coupled to a single mode of the cavity field of frequency ω_c and is also assumed to be driven by an external (classical) laser field of frequency ω_L—the cavity and laser field frequencies will be chosen so as to drive Raman transitions that couple neighbouring vibrational levels of the external motion. The physical set-up and excitation scheme are depicted in figure 1. The cavity is aligned along the x-axis, while the laser field is incident from a direction in the y–z plane (i.e. perpendicular to the x-axis).

The Hamiltonian describing the internal and external atomic degrees of freedom plus the atom–cavity and atom–laser couplings takes the form (in a frame rotating at the laser frequency)

$$\begin{aligned}\hat{H}_0 = &\sum_{j=x,y,z} \hbar\nu_j(\hat{b}_j^\dagger\hat{b}_j + \tfrac{1}{2}) + \hbar\delta\hat{a}^\dagger\hat{a} + \hbar\Delta\hat{\sigma}_+\hat{\sigma}_- \\ &+\hbar[\mathcal{E}_L(\hat{y},\hat{z},t)\hat{\sigma}_+ + \mathcal{E}_L(\hat{y},\hat{z},t)^*\hat{\sigma}_-] \\ &+\hbar g_0\sin(k\hat{x})(\hat{a}^\dagger\hat{\sigma}_- + \hat{\sigma}_+\hat{a}). \end{aligned} \quad (1)$$

Here, $\{\nu_x, \nu_y, \nu_z\}$ are the harmonic oscillation frequencies along the principal axes of the trap, $\hat{b}_j$ and $\hat{a}$ are annihilation

1464-4266/99/040496+09$30.00

operators for the quantized atomic motion and cavity field, respectively, $\hat{\sigma}_- = |g\rangle\langle e|$ is the atomic lowering operator, and $\delta = \omega_c - \omega_L$ and $\Delta = \omega_a - \omega_L$. The quantity $\mathcal{E}_L(\hat{y}, \hat{z}, t)$ is the (possibly time-dependent) amplitude of the laser field; note again that we assume that this field has no spatial dependence along the x direction. Finally, the single-photon atom–cavity dipole coupling strength is given by g_0, while the sine function describes the standing-wave structure of the cavity field (we assume that the centre of the trap is located at a *node* of the cavity field), with $k = 2\pi/\lambda$ the wavenumber of the field and $\hat{x} = [\hbar/(2m\nu_x)]^{1/2}(\hat{b}_x + \hat{b}_x^\dagger)$.

Allowing for cavity damping and atomic spontaneous emission, quantum Langevin equations for the system operators can be derived straightforwardly. For the moment, however, we ignore the effects of atomic spontaneous emission on the grounds that the detunings of the laser and cavity fields from the atomic transition frequency are very large, and hence that population of the excited atomic state $|e\rangle$ is negligible (we return to the effects of spontaneous emission in the discussion at the end of the paper). On this basis, we are also able to adiabatically eliminate the internal atomic dynamics from the problem.

We also ignore any forms of motional decoherence or heating associated with imperfections in the trap itself [12] on the basis that such effects occur on a timescale that is slow compared with the operations we consider. Again, we return to this point and discuss it more quantitatively at the end of the paper.

Finally, we assume that the size of the harmonic trap (in all directions) is small compared with the optical wavelength; under these conditions, we can make the approximation $\sin(k\hat{x}) \simeq \eta_x(\hat{b}_x + \hat{b}_x^\dagger)$, where η_x ($\ll 1$) is the Lamb–Dicke parameter. Given this assumption, it is also possible to design a configuration for which we can neglect all position dependence in the laser field†; that is, we can assume a situation where $\mathcal{E}_L(\hat{y}, \hat{z}, t) \simeq \mathcal{E}_L(t)e^{-i\phi_L}$ (with $\mathcal{E}_L(t)$ a real quantity). Henceforth, the problem essentially becomes one-dimensional and we can restrict our attention to just the x direction.

To first order in η_x, equations of motion for the operators $\hat{a}$ and $\hat{b}_x$ then follow as

$$\dot{\hat{a}} = -(\kappa + i\delta)\hat{a} + i\frac{g_0\eta_x\mathcal{E}_L(t)e^{-i\phi_L}}{\Delta}(\hat{b}_x + \hat{b}_x^\dagger) - \sqrt{2\kappa}\hat{a}_{in}(t), \quad (2)$$

$$\dot{\hat{b}}_x = -i\nu_x\hat{b}_x + i\frac{g_0\eta_x\mathcal{E}_L(t)}{\Delta}(\hat{a}^\dagger e^{-i\phi_L} + \hat{a}e^{i\phi_L}), \quad (3)$$

where κ is the decay rate of the cavity field and $\hat{a}_{in}(t)$ is a quantum noise operator describing the input to the cavity field and satisfying the commutation relation $[\hat{a}_{in}(t), \hat{a}_{in}^\dagger(t')] = \delta(t - t')$.

We now make the transformation $\hat{b}_x = e^{-i\nu_x t}\tilde{b}_x$, $\hat{a} = e^{-i\nu_x t}\tilde{a}$, and choose $\delta = \nu_x$ (i.e. tune to the 'first lower sideband'). Assuming that $\nu_x \gg \kappa$, $|(g_0\eta_x/\Delta)\mathcal{E}_L(t)|$, and $|\dot{\mathcal{E}}_L(t)/\mathcal{E}_L(t)|$, the oscillating terms in the resulting equations may be dropped in a rotating-wave approximation to yield

$$\dot{\tilde{a}} = -\kappa\tilde{a} + i\frac{g_0\eta_x\mathcal{E}_L(t)e^{-i\phi_L}}{\Delta}\tilde{b}_x - \sqrt{2\kappa}\tilde{a}_{in}(t) \quad (4)$$

† For example, if the laser field forms a standing wave with the trap centred at an *antinode*, i.e. by choosing $\mathcal{E}_L(\hat{y}, \hat{z}) \propto \cos(k\hat{y}) \sim 1$ for $\eta_y \ll 1$.

$$\dot{\tilde{b}}_x = i\frac{g_0\eta_x\mathcal{E}_L(t)}{\Delta}\tilde{a}e^{i\phi_L}. \quad (5)$$

These equations simply describe a pair of coupled harmonic oscillators, one of which is damped. In terms of a Hamiltonian, the coupling is given by (defining $\Omega(t) = -g_0\eta_x\mathcal{E}_L(t)/\Delta$ (real))

$$\tilde{H}(t) = \hbar\Omega(t)(\tilde{a}^\dagger\tilde{b}_x e^{-i\phi_L} + \tilde{b}_x^\dagger\tilde{a}e^{i\phi_L}), \quad (6)$$

a result derived by Zeng and Lin [13].

3. Quantum state transfer

As pointed out by Zeng and Lin [13], when cavity losses can be neglected the above coupling enables complete (pure or mixed) state transfer between the atomic motion and the cavity light field. For example, given a finite laser pulse duration, and assuming for simplicity that $\mathcal{E}_L(t)$ is a real and positive function of time, then solutions for $\tilde{a}(t = +\infty) \equiv \tilde{a}(+\infty)$ and $\tilde{b}_x(t = +\infty) \equiv \tilde{b}_x(+\infty)$ can be derived as

$$\tilde{a}(+\infty) = \tilde{a}(-\infty)\cos\theta - ie^{-i\phi_L}\tilde{b}_x(-\infty)\sin\theta \quad (7)$$

$$\tilde{b}_x(+\infty) = -ie^{i\phi_L}\tilde{a}(-\infty)\sin\theta + \tilde{b}_x(-\infty)\cos\theta, \quad (8)$$

where $\theta = \int_{-\infty}^{\infty}\Omega(\tau)\,d\tau$. Choosing $\theta = (N + \frac{1}{2})\pi$, with N an integer, and $\phi_L = \pi/2$ yields

$$\tilde{a}(+\infty) = \mp\tilde{b}_x(-\infty), \qquad \tilde{b}_x(+\infty) = \pm\tilde{a}(-\infty), \quad (9)$$

from which it follows that, given an initial vacuum state of the field, *any initial state of the motion can be transferred one-to-one to the state of the cavity field* and the motion is reduced to its ground state (other examples of this kind of state exchange between harmonic oscillator modes are available‡).

3.1. Underdamped regime

The result derived above demonstrating the possibility of complete state transfer between the quantized atomic motion and the cavity field mode obviously offers some very interesting further possibilities. If the damping of the cavity mode is sufficiently weak, then one can imagine a situation in which a suitable laser pulse is applied so as to transfer a motional state to the cavity mode (in a time short compared with κ^{-1}), after which the cavity field is allowed to decay. Making homodyne measurements on the output field from the cavity and using the well-established method of optical homodyne tomography [18, 19], the density matrix of the cavity field mode, and hence of the initial motional state, could be reconstructed from many repeated cycles of preparation and measurement.

Given that the motion is always left in its ground state after the laser pulse, this can also be seen as a novel means of cooling, or 'resetting,' the atomic motion in a single operation§. Of course, in the regime of operation that we

‡ The authors of [16] consider the case in which two vibrational degrees of freedom of a trapped ion are linearly coupled via laser-induced Raman transitions. The authors of [17] consider the case of charged particle traps coupled through their endcaps; this leads to a linear coupling between the vibrational modes of the trapped particles.

§ This follows the same principle as proposed in [17] for cooling a source mode to its zero-point state by transferring its excitation to, in their case, a trapped ion, which is then cooled using sideband cooling.

are assuming (the resolved sideband limit), conventional sideband cooling (using atomic spontaneous emission) would also be an efficient means of cooling the motion to the ground state.

3.2. Overdamped regime

The opposite limit, in which κ is large compared with the magnitude of the effective coupling rate $\Omega(t)$ (but, of course, still small compared with the trap frequency ν_x) is actually of more interest to us and indeed allows further simplification of the model. In particular, we can consider adiabatically eliminating the cavity mode from the dynamics, i.e., setting $\dot{\tilde{a}} = 0$ and substituting

$$\tilde{a} \simeq -\frac{\Omega(t)}{\kappa}\tilde{b}_x - \sqrt{2/\kappa}\tilde{a}_{\rm in}(t) \tag{10}$$

into the equation for $\dot{\tilde{b}}_x$ to give

$$\begin{aligned}\dot{\tilde{b}}_x &\simeq -\frac{[\Omega(t)]^2}{\kappa}\tilde{b}_x + \Omega(t)\sqrt{2/\kappa}\tilde{a}_{\rm in}(t)\\ &\equiv -\Gamma(t)\tilde{b}_x + \sqrt{2\Gamma(t)}\tilde{a}_{\rm in}(t),\end{aligned} \tag{11}$$

where we have set $\phi_{\rm L} = \pi/2$ for simplicity.

This equation simply describes a quantum harmonic oscillator subject to damping at the (possibly time-dependent) rate $\Gamma(t)$. In the case of a vacuum cavity input field, it obviously models sideband cooling to the ground state due to a form of cavity-induced spontaneous emission [20, 21].

3.2.1. Driven cavity: light-to-motion state transfer. However, one can also consider different kinds of inputs to the cavity field, i.e., choices of the input field operator $\tilde{a}_{\rm in}(t)$ that give rise to nontrivial input field statistics. This is of interest because, given the simple linear form of (11), it follows that the statistics of the input field can be 'written onto' the state of the oscillator. In particular, assuming that $\Gamma(t) = \Gamma$, a constant, then in frequency space the solution to (11) is simply

$$\tilde{b}_x(\omega) = \frac{\sqrt{2\Gamma}\tilde{a}_{\rm in}(\omega)}{-{\rm i}\omega + \Gamma}. \tag{12}$$

For example, the input field could be an *ideal quantum squeezed vacuum* as derived from the output of a degenerate parametric amplifier [22, 23]. If the squeezing happens to be broadband (with respect to the characteristic rates associated with the system upon which it is incident), then the appropriate input field correlation functions can be written in the forms [24]

$$\langle \tilde{a}^\dagger_{\rm in}(\omega)\tilde{a}_{\rm in}(\omega')\rangle = N\delta(\omega - \omega') \tag{13}$$

$$\langle \tilde{a}_{\rm in}(\omega)\tilde{a}_{\rm in}(\omega')\rangle = M\delta(\omega + \omega'), \tag{14}$$

with $M = |M|{\rm e}^{{\rm i}\theta}$ and $|M|^2 = N(N+1)$. Given such an input, the system is equivalently described by the master equation [24]

$$\begin{aligned}\dot{\rho}_{\rm m} = {}&\Gamma(N+1)(2\tilde{b}_x\rho_{\rm m}\tilde{b}^\dagger_x - \tilde{b}^\dagger_x\tilde{b}_x\rho_{\rm m} - \rho_{\rm m}\tilde{b}^\dagger_x\tilde{b}_x)\\ &+\Gamma N(2\tilde{b}^\dagger_x\rho_{\rm m}\tilde{b}_x - \tilde{b}_x\tilde{b}^\dagger_x\rho_{\rm m} - \rho_{\rm m}\tilde{b}_x\tilde{b}^\dagger_x)\\ &-\Gamma M(2\tilde{b}_x\rho_{\rm m}\tilde{b}_x - \tilde{b}_x\tilde{b}_x\rho_{\rm m} - \rho_{\rm m}\tilde{b}_x\tilde{b}_x)\\ &-\Gamma M^*(2\tilde{b}^\dagger_x\rho_{\rm m}\tilde{b}^\dagger_x - \tilde{b}^\dagger_x\tilde{b}^\dagger_x\rho_{\rm m} - \rho_{\rm m}\tilde{b}^\dagger_x\tilde{b}^\dagger_x),\end{aligned} \tag{15}$$

where $\rho_{\rm m}$ is the density operator for the motion of the trapped atom. In steady state, the density operator is that of an ideal squeezed state, that is

$$\rho^{\rm ss}_{\rm m} = \hat{S}|0\rangle\langle 0|\hat{S}^+, \tag{16}$$

where $\hat{S}$ is the squeezing operator [25], i.e. $\hat{S}\tilde{b}\hat{S}^+ = \mu\tilde{b}_x + \nu\tilde{b}^\dagger_x$ with $\mu = (N+1)^{1/2}$ and $\nu = N^{1/2}{\rm e}^{{\rm i}\theta}$.

There are, of course, other ways of preparing such nonclassical states of the motion which have indeed already been implemented experimentally [1–3]. These preparations have typically employed pulsed *classical* light fields to facilitate the required motional state transformations. The above scheme is novel in that it involves the direct transfer of statistics from a *nonclassical* continuous-wave light field to the motional state of the trapped atom.

3.2.2. Numerical calculations. To numerically model state transfer between light and motion in the overdamped regime described above, we consider, as above, the cavity mode to be resonantly driven by squeezed light from a degenerate parametric oscillator, as illustrated in figure 2. For our simulations, we include the dynamics of the parametric oscillator using the cascaded systems formalism developed in [26, 27] (further applications of the formalism are given in [28]). In particular, we model our system with the master equation

$$\begin{aligned}\dot{\rho} = {}&-\frac{\rm i}{\hbar}[\tilde{H}_{ab}(t) + \tilde{H}_c, \rho] + \kappa_a(2\tilde{a}\rho\tilde{a}^\dagger - \tilde{a}^\dagger\tilde{a}\rho - \rho\tilde{a}^\dagger\tilde{a})\\ &+\kappa_c(2\tilde{c}\rho\tilde{c}^\dagger - \tilde{c}^\dagger\tilde{c}\rho - \rho\tilde{c}^\dagger\tilde{c})\\ &-2\sqrt{\kappa_a\kappa_c}([\tilde{a}^\dagger, \tilde{c}\rho] + [\rho\tilde{c}^\dagger, \tilde{a}]).\end{aligned} \tag{17}$$

Here, $\tilde{H}_{ab}(t)$ describes the effective coupling between the vibrational motion of the trapped atom and the cavity light field as derived above. However, in addition we retain the rotating, or nonsecular terms, i.e., we take

$$\begin{aligned}\tilde{H}_{ab}(t) = {}&\hbar\Omega(\tilde{a}^\dagger\tilde{b}_x{\rm e}^{-{\rm i}\phi_{\rm L}} + \tilde{b}^\dagger_x\tilde{a}{\rm e}^{{\rm i}\phi_{\rm L}})\\ &+\hbar\Omega(\tilde{a}^\dagger\tilde{b}^\dagger_x{\rm e}^{-{\rm i}\phi_{\rm L}+2i\nu_x t} + \tilde{a}\tilde{b}_x{\rm e}^{{\rm i}\phi_{\rm L}-2i\nu_x t}).\end{aligned} \tag{18}$$

The coupling parameter Ω is assumed to be a constant. The Hamiltonian $\tilde{H}_c$ models the parametric oscillator (driven below threshold), taking the form

$$\tilde{H}_c = \tfrac{1}{2}{\rm i}\hbar[\epsilon^*\tilde{c}^2 - \epsilon(\tilde{c}^\dagger)^2], \tag{19}$$

where $\tilde{c}$ is the annihilation operator for the cavity mode of the parametric oscillator and $\epsilon = |\epsilon|{\rm e}^{{\rm i}\theta}$ is the amplitude of the coherent field driving the oscillator. The linewidth of the (one-sided) parametric oscillator cavity mode is κ_c. Finally, the last term in (17) describes the (unidirectional) coupling of the incoming squeezed light to the cavity mode. This coupling is assumed to be ideal.

By using a truncated state basis, the master equation (17) is numerically propagated until a steady state is achieved. In fact, due to the time-dependent terms in $\tilde{H}_{ab}(t)$, only a quasi-steady state can in principle be achieved, but for the parameters we consider only a very weak time-dependence (i.e. a weak modulation) occurs. The elements of the reduced density matrix of the motional mode in the steady state ($\rho^{\rm sim}_{\rm m}$) are shown in figure 3 for the choice of parameters

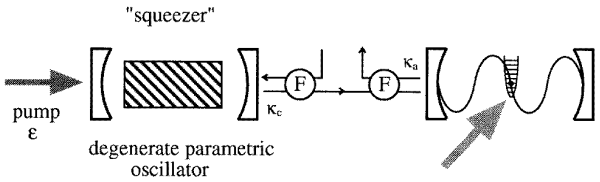

Figure 2. Schematic of the cascaded system for transfer of statistics from a squeezed light field to the motional state of a trapped atom. Faraday isolators (F) facilitate a unidirectional coupling between the squeezed light source and the atom–cavity system.

$\nu_x/\kappa_a = 10$, $\Omega/\kappa_a = 0.1$, $\kappa_c/\kappa_a = 1$ and $\epsilon/\kappa_c = 0.3$ (corresponding to 71% maximum squeezing in the input light field). These parameters are in the regime for which the master equation (15) should be valid and, indeed, we find the steady state of the motion to be approached on a timescale $\Gamma^{-1} = (\Omega^2/\kappa_a)^{-1} = 100\kappa_a^{-1}$. Characteristic squeezed state features are evident in the figure (e.g. only even number states are populated) and the fidelity with which the predicted ideal squeezed state is achieved is computed to be $\langle 0|\hat{S}^+\rho_{\rm m}^{\rm sim}\hat{S}|0\rangle \simeq 0.99$ for the appropriate values of N and M in the theory.

3.3. Entanglement transfer from light fields to separated trapped atoms

The scheme outlined above can be extended to the transfer of quantum mechanical entanglement from light fields to motional states of two or more trapped atoms at physically separated sites. Consider, for example, the pair of output fields from a *nondegenerate parametric amplifier* (the fields may be nondegenerate in polarization or in frequency) [22]. At the output from the parametric amplifier, these fields could be separated in space and then made to impinge upon two cavities containing trapped atoms in the configuration described above. The quantum mechanical correlations that exist between the two light fields generated by parametric downconversion could thus be transferred (in steady state) to correlations between motional states of trapped atoms at two distinct sites.

3.4. Quantum teleportation of motional states

An exciting recent development in the field of quantum communication has been the experimental investigation of schemes for the teleportation of quantum states [29–31]. Of particular interest in the present context is the demonstration by Furusawa *et al* [31] of unconditional quantum teleportation of optical coherent states using squeezed-state fields and entanglement of the sort discussed above. By incorporating cavities containing trapped ions in the state transfer configuration of this work (in the bad cavity limit), it should be possible to employ the scheme of [31] for the teleportation of *motional* states.

In particular, a motional state could be 'mapped' onto a light field which enters the configuration of [31] at the 'sending' station. This field is teleported to a 'receiving' station where it is made to impinge upon a second trapped-ion plus cavity system in the state transfer configuration. The teleported light field is thus mapped onto the motional mode of the second trapped ion and teleportation of the motional state is completed. We will examine teleportation of motional states in more detail in a future paper.

3.5. Motion-to-light state transfer: generation of nonclassical output light fields

Given the variety of, and efficiency with which, nonclassical motional states of single trapped atoms have been experimentally realized [1–3], it is worth noting the potential of our scheme as a *source* of nonclassical output light fields. The output light field is related to the input and internal cavity fields by [24, 25]

$$\tilde{a}_{\rm out}(t) = \tilde{a}_{\rm in}(t) + \sqrt{2\kappa}\tilde{a}(t), \tag{20}$$

which in the overdamped limit becomes (using (10))

$$\tilde{a}_{\rm out}(t) \simeq -\tilde{a}_{\rm in}(t) - \sqrt{2\Gamma(t)}\tilde{b}_x(t), \tag{21}$$

where we assume that $\Omega(t) \geqslant 0$. Hence, given a vacuum field input to the cavity, the output field is determined by the motional state of the trapped atom. Further, depending on the nature of the motional state preparation, the output may be pulsed *or* continuous; for a continuous output one would have $\Gamma(t) = \Gamma$, a constant, and the motional state preparation scheme would have to operate in a continuous manner also. As an example, consider squeezed motional states, which may be generated by applying an electric field gradient with a frequency $2\nu_x$ to the ion [17], or by irradiating the ion with two laser beams differing in frequency by $2\nu_x$ [1].

Note that in [1] squeezed states of the motion were produced exhibiting a reduction in the variance of the squeezed quadrature by a factor of 40. Such quadrature noise reduction has yet to be approached via traditional optical means, suggesting that the present state transfer configuration is worthy of further investigation†.

4. Transfer of a motional state between separated trapped atoms

Recently, Cirac *et al* [32] (see also [33–35]) demonstrated how quantum transmission of a qubit between two nodes of a quantum network can be implemented in a physical system using light as the carrier of the quantum information. In particular, they showed how the transformation

$$(c_0|0\rangle_1 + c_1|1\rangle_1) \otimes |0\rangle_2 \rightarrow |0\rangle_1 \otimes (c_0|0\rangle_2 + c_1|1\rangle_2) \tag{22}$$

can be achieved where $|0\rangle_1$ and $|1\rangle_1$ are internal states of an atom at node 1 and $|0\rangle_2$ and $|1\rangle_2$ are the corresponding states of a second atom at (the spatially separated) node 2. At each node, the atom is located within a cavity supporting a single mode of the electromagnetic field, with which it is made to undergo a controlled time-dependent interaction via a laser-assisted Raman process. With suitably chosen laser pulses at the two nodes, the transmission described by (22) can be

† Note, however, that large squeezing implies population of large-n number states and a broader spread of the atomic wavefunction, which makes the Lamb–Dicke assumption of our scheme more restrictive.

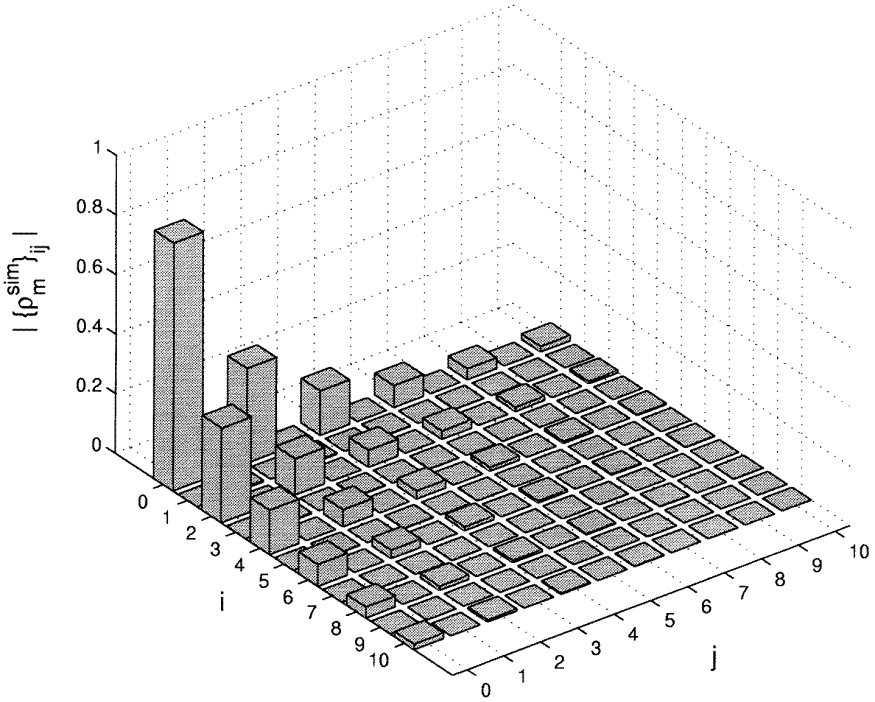

Figure 3. Elements of the steady-state reduced density matrix of the motional mode of the trapped atom when the cavity mode is driven by quadrature squeezed light from a degenerate parametric oscillator. Parameters are given in the text.

faithfully reproduced, facilitated by the transfer of a *photon* wavepacket between the two nodes.

In the same spirit, here we consider the transmission of *arbitrary motional states* of trapped atoms between two distinct sites, facilitated once again by cavity light fields and photon wavepackets. We consider two separated atom–cavity arrangements, each in the configuration described in section 2, so that the combined system Hamiltonian can be written as

$$\tilde{H} = \hbar\Omega_1(t)(\tilde{a}_1^\dagger \tilde{b}_1 \mathrm{e}^{-\mathrm{i}\phi_1} + \tilde{b}_1^\dagger \tilde{a}_1 \mathrm{e}^{\mathrm{i}\phi_1}) + \hbar\Omega_2(t)(\tilde{a}_2^\dagger \tilde{b}_2 \mathrm{e}^{-\mathrm{i}\phi_2} + \tilde{b}_2^\dagger \tilde{a}_2 \mathrm{e}^{\mathrm{i}\phi_2}), \quad (23)$$

where the subscripts $\{1, 2\}$ denote the site of each atom or cavity mode and we now omit the subscript x for simplicity.

4.1. Cascaded systems model

The two cavity modes are each damped at rate κ, but coupling between their external fields is assumed to be unidirectional. In particular, the output from cavity 1 is incident upon (i.e. provides the input field to) cavity 2, but not vice versa. Such a situation is depicted in figure 4 and is again modelled by the cascaded systems formalism introduced earlier [26, 27]. In this formalism, the master equation for our system is derived in the form

$$\dot{\rho} = (\mathcal{L}_0 + \mathcal{L}_c)\rho, \quad (24)$$

where $\mathcal{L}_0\rho = -(\mathrm{i}/\hbar)[\tilde{H}, \rho]$ and

$$\mathcal{L}_c\rho = \kappa(2\tilde{a}_1\rho\tilde{a}_1^\dagger - \tilde{a}_1^\dagger\tilde{a}_1\rho - \rho\tilde{a}_1^\dagger\tilde{a}_1) + \kappa(2\tilde{a}_2\rho\tilde{a}_2^\dagger - \tilde{a}_2^\dagger\tilde{a}_2\rho - \rho\tilde{a}_2^\dagger\tilde{a}_2) - 2\kappa([\tilde{a}_2^\dagger, \tilde{a}_1\rho] + [\rho\tilde{a}_1^\dagger, \tilde{a}_2]), \quad (25)$$

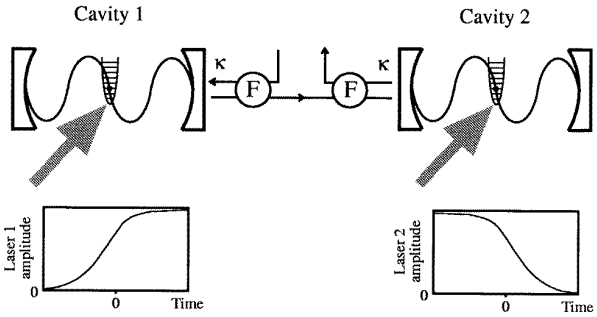

Figure 4. Schematic of the cascaded system for transfer of a motional state between separated trapped atoms/ions. The input to the first cavity is ordinary vacuum and Faraday isolators (F) facilitate a unidirectional coupling between the first and second cavities.

where a vacuum input to the first cavity has been assumed. The last term in (25) provides the desired unidirectional coupling in the theory.

To simplify the model, we assume, as before, that the decay rate κ is large compared with other rates in the system (apart from the trap frequency ν) and that the cavity fields can be adiabatically eliminated from the system dynamics. In the approach we are following in this section, this leads to a reduced master equation for the density operator of the motion of the two atoms, given formally by [24]

$$\dot{\rho}_m = \mathrm{Tr}_c\left\{\mathcal{L}_0 \int_0^\infty \mathrm{d}\tau\, \mathrm{e}^{\mathcal{L}_c\tau}\mathcal{L}_0\rho_c^{ss}\right\}\rho_m, \quad (26)$$

where ρ_c^{ss} is the steady state density matrix for the two cavity modes. To evaluate this expression explicitly requires steady state correlation functions for the operators $\tilde{a}_1$ and $\tilde{a}_2$,

which can be derived from (25) using the quantum regression theorem. As shown in the appendix, the only nonzero correlation functions are

$$\langle\tilde{a}_1(\tau)\tilde{a}_1^\dagger(0)\rangle_{\rm ss} = \langle\tilde{a}_2(\tau)\tilde{a}_2^\dagger(0)\rangle_{\rm ss} = {\rm e}^{-\kappa\tau} \tag{27}$$

and

$$\langle\tilde{a}_1(0)\tilde{a}_2^\dagger(\tau)\rangle_{\rm ss} = \langle\tilde{a}_2(\tau)\tilde{a}_1^\dagger(0)\rangle_{\rm ss} = -2\kappa\tau{\rm e}^{-\kappa\tau}. \tag{28}$$

Using these expressions gives

$$\begin{aligned}\dot{\rho}_{\rm m} = {}&\Gamma_1(t)(2\tilde{b}_1\rho_{\rm m}\tilde{b}_1^\dagger - \tilde{b}_1^\dagger\tilde{b}_1\rho_{\rm m} - \rho_{\rm m}\tilde{b}_1^\dagger\tilde{b}_1)\\ &+\Gamma_2(t)(2\tilde{b}_2\rho_{\rm m}\tilde{b}_2^\dagger - \tilde{b}_2^\dagger\tilde{b}_2\rho_{\rm m} - \rho_{\rm m}\tilde{b}_2^\dagger\tilde{b}_2)\\ &+2\sqrt{\Gamma_1(t)\Gamma_2(t)}\{[\tilde{b}_2^\dagger, \tilde{b}_1\rho_{\rm m}]{\rm e}^{-{\rm i}(\phi_1-\phi_2)}\\ &+[\rho_{\rm m}\tilde{b}_1^\dagger, \tilde{b}_2]{\rm e}^{{\rm i}(\phi_1-\phi_2)}\}.\end{aligned} \tag{29}$$

This master equation once again describes a cascaded system, only now the 'coupling' appears directly between the motional modes of the two atoms.

4.2. Quantum trajectories and ideal state transmission

To demonstrate the transmission properties of the coupled system, we again follow Cirac *et al* and employ the technique of quantum trajectories [27, 36]. This technique simulates a given master equation by propagating a system wavefunction $|\psi(t)\rangle$ subject to a non-Hermitian effective Hamiltonian. This propagation is interrupted at random times $\{t_r\}$ by wavefunction collapses, or quantum jumps, $|\psi(t_r + {\rm d}t)\rangle = \tilde{C}|\psi(t)\rangle$, which can be interpreted as, in our particular instance, the emission and destructive detection of photons from the cavity fields.

For the master equation derived above, the effective Hamiltonian takes the form (choosing the laser phases such that $\phi_1 = \phi_2$)

$$\tilde{H}_{\rm eff}(t) = -{\rm i}\Gamma_1(t)\tilde{b}_1^\dagger\tilde{b}_1 - {\rm i}\Gamma_2(t)\tilde{b}_2^\dagger\tilde{b}_2 + 2{\rm i}\sqrt{\Gamma_1(t)\Gamma_2(t)}\tilde{b}_2^\dagger\tilde{b}_1, \tag{30}$$

while the collapse operator is given by

$$\tilde{C} = \sqrt{\Gamma_1(t)}\tilde{b}_1 - \sqrt{\Gamma_2(t)}\tilde{b}_2. \tag{31}$$

The basic idea is to design laser pulse profiles (manifest through $\Gamma_i(t)$) at the two sites such that the ideal quantum transmission

$$\sum_{n=0}^{\infty} c_n|n\rangle_1 \otimes |0\rangle_2 \to |0\rangle_1 \otimes \sum_{n=0}^{\infty} c_n|n\rangle_2, \tag{32}$$

can be achieved. Here $|n\rangle_i$ denotes the nth Fock state of the motion of atom i. A necessary condition for successful transmission is that a quantum jump never occurs, i.e. $\tilde{C}|\psi(t)\rangle = 0$ for all t, in which case the effective Hamiltonian becomes a Hermitian operator. This can be interpreted in terms of transfer via a *dark* state of the cascaded system.

We expand the state of the system as

$$|\psi(t)\rangle = \sum_{n=0}^{\infty} c_n \sum_{m=0}^{n} \alpha_m^{(n)}(t)|n-m\rangle_1 \otimes |m\rangle_2, \tag{33}$$

with initial condition

$$\alpha_0^{(n)}(-\infty) = 1, \qquad \alpha_{m\neq 0}^{(n)}(-\infty) = 0, \tag{34}$$

and normalization

$$\sum_{m=0}^{n} |\alpha_m^{(n)}(t)|^2 = 1. \tag{35}$$

For ideal quantum transmission, one requires that

$$\alpha_n^{(n)}(+\infty) = \alpha_0^{(n)}(-\infty) = 1. \tag{36}$$

Equations of motion for the $\{\alpha_m^{(n)}(t)\}$ are derived using (30) and (33); the equations for the $m = 0$ components take the simple closed form

$$\dot{\alpha}_0^{(n)}(t) = -n\Gamma_1(t)\alpha_0^{(n)}(t), \tag{37}$$

with solutions

$$\alpha_0^{(n)}(t) = \exp\left\{-n\int_{-\infty}^{t}\Gamma_1(t')\,{\rm d}t'\right\}. \tag{38}$$

Now, applying the dark state condition

$$\left\{\sqrt{\Gamma_1(t)}\tilde{b}_1 - \sqrt{\Gamma_2(t)}\tilde{b}_2\right\}|\psi(t)\rangle = 0 \tag{39}$$

yields the sequence of straightforward algebraic equations

$$\begin{aligned}\sqrt{n\Gamma_1(t)}\alpha_0^{(n)}(t) - \sqrt{\Gamma_2(t)}\alpha_1^{(n)}(t) &= 0,\\ \sqrt{(n-1)\Gamma_1(t)}\alpha_1^{(n)}(t) - \sqrt{2\Gamma_2(t)}\alpha_2^{(n)}(t) &= 0,\\ \sqrt{(n-2)\Gamma_1(t)}\alpha_2^{(n)}(t) - \sqrt{3\Gamma_2(t)}\alpha_3^{(n)}(t) &= 0, \ldots,\end{aligned} \tag{40}$$

from which a solution for $\alpha_m^{(n)}(t)$ in terms of $\alpha_0^{(n)}(t)$ follows as

$$\alpha_m^{(n)}(t) = \left[\frac{\Gamma_1(t)}{\Gamma_2(t)}\right]^{m/2}\sqrt{\frac{n!}{m!(n-m)!}}\alpha_0^{(n)}(t). \tag{41}$$

Applying the normalization condition gives

$$\sum_{m=0}^{n}[\alpha_m^{(n)}(t)]^2 = \left[1 + \frac{\Gamma_1(t)}{\Gamma_2(t)}\right]^n[\alpha_0^{(n)}(t)]^2 = 1 \tag{42}$$

and thus

$$\frac{\Gamma_1(t)}{\Gamma_2(t)} = \exp\left\{2\int_{-\infty}^{t}\Gamma_1(t')\,{\rm d}t'\right\} - 1, \tag{43}$$

which demonstrates that it is possible to choose pulse shapes of the laser fields in such a way that the perfect transmission (32) can be achieved.

We have not explored, in detail, pulse shapes satisfying (43). We do find, however, that (43) admits the following simple *analytical* solutions,

$$\Gamma_1(t) = \Gamma\frac{{\rm e}^{\Gamma t}}{{\rm e}^{\Gamma t} + {\rm e}^{-\Gamma t}}, \qquad \Gamma_2(t) = \Gamma_1(-t), \tag{44}$$

with the limits $\Gamma_1(t) \to 0$ (Γ) as $t \to -\infty(+\infty)$, and vice versa for $\Gamma_2(t)$. We use these forms in the numerical calculations that follow.

4.3. Numerical calculations

For the purpose of numerical calculations, we retain the dynamics of the cavity field modes and solve the cascaded systems master equation

$$\dot{\rho} = -\frac{\mathrm{i}}{\hbar}[\tilde{H}_1(t) + \tilde{H}_2(t), \rho] + \kappa(2\tilde{a}_1\rho\tilde{a}_1^\dagger - \tilde{a}_1^\dagger\tilde{a}_1\rho - \rho\tilde{a}_1^\dagger\tilde{a}_1) + \kappa(2\tilde{a}_2\rho\tilde{a}_2^\dagger - \tilde{a}_2^\dagger\tilde{a}_2\rho - \rho\tilde{a}_2^\dagger\tilde{a}_2) - 2\kappa([\tilde{a}_2^\dagger, \tilde{a}_1\rho] + [\rho\tilde{a}_1^\dagger, \tilde{a}_2]) \quad (45)$$

with

$$\tilde{H}_k(t) = \hbar\Omega_k(t)(\tilde{a}_k^\dagger\tilde{b}_k\mathrm{e}^{-\mathrm{i}\phi_k} + \tilde{b}_k^\dagger\tilde{a}_k\mathrm{e}^{\mathrm{i}\phi_k}) + \hbar\Omega_k(t)(\tilde{a}_k^\dagger\tilde{b}_k^\dagger\mathrm{e}^{-\mathrm{i}\phi_k+2\mathrm{i}\nu t} + \tilde{a}_k\tilde{b}_k\mathrm{e}^{\mathrm{i}\phi_k-2\mathrm{i}\nu t}), \quad (46)$$

where $k = 1, 2$. Once again, we include the rotating terms $\tilde{a}_k\tilde{b}_k$ and $\tilde{a}_k^\dagger\tilde{b}_k^\dagger$, while the forms of the time-dependent effective coupling parameters $\Omega_1(t)$ and $\Omega_2(t)$ are chosen in accordance with the work of the previous section, i.e.,

$$\Omega_1(t) = \Omega\sqrt{\frac{\mathrm{e}^{\Gamma t}}{\mathrm{e}^{\Gamma t} + \mathrm{e}^{-\Gamma t}}} = \Omega_2(-t), \quad (47)$$

where $\Gamma = \Omega^2/\kappa$ (and we choose $\phi_1 = \phi_2 = 0$).

As the state to be transferred, we choose, arbitrarily (in practice we are somewhat limited by the size of the basis set we can use comfortably in our simulations),

$$|\psi\rangle = \tfrac{1}{2}(|0\rangle + \mathrm{e}^{\mathrm{i}\pi/3}|1\rangle + \mathrm{e}^{\mathrm{i}2\pi/3}|2\rangle + \mathrm{e}^{\mathrm{i}\pi}|3\rangle), \quad (48)$$

so that the initial state of the total system is $|0\rangle_{a1} \otimes |\psi\rangle_{b1} \otimes |0\rangle_{a2} \otimes |0\rangle_{b2}$, while the target state is

$$|\psi_{\mathrm{target}}\rangle = |0\rangle_{a1} \otimes |0\rangle_{b1} \otimes |0\rangle_{a2} \otimes |\psi\rangle_{b2}. \quad (49)$$

The transmission fidelity, which we define by

$$F(t) = \langle\psi_{\mathrm{target}}|\rho(t)|\psi_{\mathrm{target}}\rangle, \quad (50)$$

is plotted in figure 5 for $\Omega/\kappa = 0.141$ (corresponding to $\Gamma/\kappa = 0.02$) and three different values of the trap frequency ν. Note that the initial value of the fidelity is finite due to the contribution from $|0\rangle$ in the state $|\psi\rangle$. For $\nu/\kappa = 20$ (10) the state is transmitted with a fidelity of 0.995 (0.980). As ν/κ is lowered the fidelity is reduced as the rotating terms in the effective Hamiltonians $\tilde{H}_k(t)$ begin to contribute more strongly to the dynamics. Nevertheless, a fidelity of 0.925 is found even for $\nu/\kappa = 5$.

In figure 6 we consider a single value of the trap frequency, $\nu/\kappa = 20$, but now vary the coupling parameter Ω, which varies the effective rate Γ of the state transfer operation. We also choose larger values of Ω compared with κ to assess how well the chosen pulse shapes drive the state transfer as the adiabatic approximation ($\kappa \gg \Omega$) ceases to be valid. As one can see, the fidelity of the transmission remains high even with $\Omega/\kappa = 0.4$ (0.984) and 0.5 (0.970), but at $\Omega/\kappa = 0.7$ deteriorates to 0.905. Notably, the timescales for the transfer are significantly faster than in the previous figure, which is possibly advantageous from an experimental point of view.

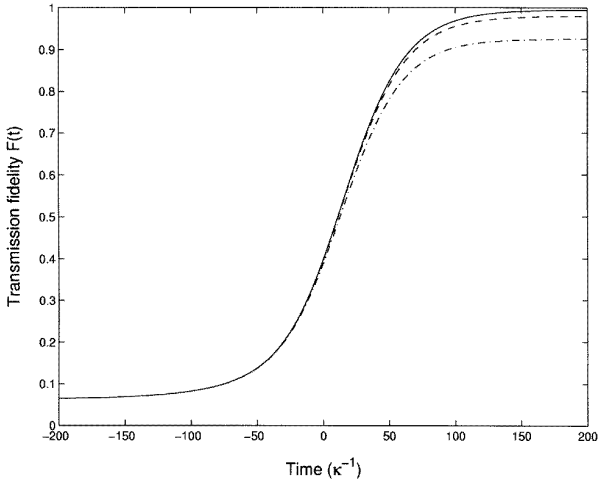

Figure 5. Fidelity of the transmission $F(t)$ for the state $|\psi\rangle$ of equation (48) using the pulse shapes (47) with $\Omega/\kappa = 0.141$ ($\Gamma/\kappa = 0.02$), and taking $\nu/\kappa = 20$ (solid curve), 10 (dashed curve) and 5 (dot-dashed curve).

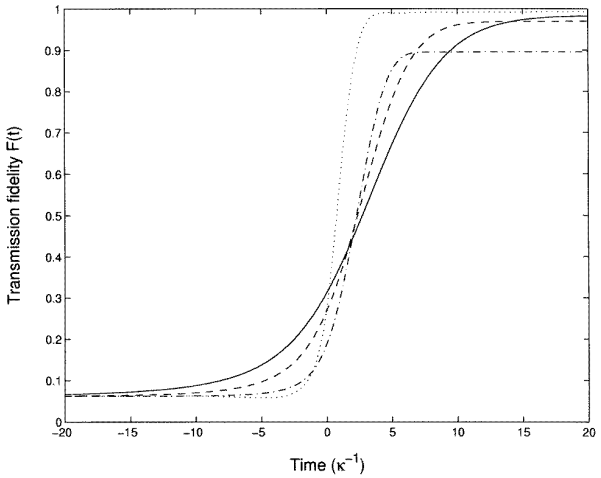

Figure 6. Fidelity of the transmission $F(t)$ for the state $|\psi\rangle$ of equation (48) for $\nu/\kappa = 20$ with $\Omega/\kappa = 0.4$ (solid curve), 0.5 (dashed curve) and 0.7 (dot-dashed curve), using the pulse shapes (47) (overdamped analysis). The dotted curve shows the result from the underdamped analysis for $\Omega/\kappa = 0.7$, using $\Omega_1(t) = \Omega$ for $t \geqslant 0$ and the form (51) for $\Omega_1(t < 0)$ [$\Omega_2(t) = \Omega_1(-t)$].

4.4. Underdamped regime

The overdamped regime considered above probably corresponds to the most likely experimental scenario. However, a situation where $\Omega > \kappa$ is still possible and could offer some further advantages in terms of transfer rates, which, in such a regime, would be of the order of κ. Of course, if $\Omega > \kappa$ then one must include the cavity modes and their dynamics in the analysis, which thereby becomes somewhat more complicated.

Nevertheless, we find that it is still possible to derive pulse shapes that allow high-fidelity transmission of arbitrary quantum states. In particular, following the kind of approach used in [32], whereby one assumes that $\Omega_1(t) = \Omega$ (a constant) for $t \geqslant 0$ and that $\Omega_2(t) = \Omega_1(-t)$ (i.e. the

symmetric pulse condition), we are able to arrive at the form

$$\Omega_1(-t) = -\frac{\Omega f(t) + 2\kappa h(t)}{\sqrt{1 - f(t)^2 - 2h(t)^2}} \qquad (t \geqslant 0), \quad (51)$$

where

$$f(t) = \frac{1}{p}(\lambda_+ e^{\lambda_- t} - \lambda_- e^{\lambda_+ t}) f(0) + \frac{\Omega}{p}(e^{\lambda_+ t} - e^{\lambda_- t}) h(0), \quad (52)$$

$$h(t) = \frac{1}{p}(\lambda_+ e^{\lambda_+ t} - \lambda_- e^{\lambda_- t}) h(0) - \frac{\Omega}{p}(e^{\lambda_+ t} - e^{\lambda_- t}) f(0), \quad (53)$$

with $\lambda_\pm = -(\frac{1}{2})(\kappa \pm p)$, $p = (\kappa^2 - 4\Omega^2)^{1/2}$, and

$$f(0) = \sqrt{\frac{\kappa^2/2}{\kappa^2 + \Omega^2}}, \qquad h(0) = -\sqrt{\frac{\Omega^2/2}{\kappa^2 + \Omega^2}}. \quad (54)$$

That such forms for the pulse shapes can successfully facilitate state transmission between the two atoms is illustrated by the dotted curve in figure 6 for the same state $|\psi\rangle$ considered above and with $\Omega/\kappa = 0.7$. The state is transmitted with a fidelity of 0.993, clearly improving on the result from the approach in the overdamped regime and also doing so on a faster timescale.

5. Discussion

In this paper we have described schemes for the transfer of quite general quantum states between light fields and atomic motion and between the motion of trapped atoms at separate sites. We now want to consider in more detail some of the basic assumptions involved in our model and to examine possible experimental situations.

Clearly, a very important assumption is that the effects of atomic spontaneous emission can be neglected. In a master equation approach, atomic spontaneous emission with the effects of recoil taken into account is modelled by a term of the form (considering motion only along the x-axis) [37]

$$\{\dot\rho\}_{\rm spon} = \frac{\gamma}{2}(2\hat\sigma_- \tilde\rho \hat\sigma_+ - \hat\sigma_+\hat\sigma_-\rho - \rho\hat\sigma_+\hat\sigma_-), \quad (55)$$

where

$$\tilde\rho = \tfrac{1}{2}\int_{-1}^{+1} {\rm d}u\, W(u) e^{{\rm i}ku\hat x}\rho e^{-{\rm i}ku\hat x} = \tfrac{1}{2}\int_{-1}^{+1} {\rm d}u\, W(u) e^{{\rm i}\eta_x(\hat b_x + \hat b_x^\dagger)}\rho e^{-{\rm i}\eta_x(\hat b_x + \hat b_x^\dagger)}. \quad (56)$$

Here, γ is the spontaneous emission rate and $W(u) = (\frac{3}{4})(1+u^2)$ describes the angular distribution of spontaneous emission for an atomic dipole transition. Incorporating this into our analysis and adiabatically eliminating the atomic and cavity degrees of freedom as before, one finds that the leading order (in η_x) contribution to the motional dynamics contributed by atomic recoil due to spontaneous emission takes the form

$$\eta_x^2 \frac{\gamma}{10}\frac{\mathcal{E}_{\rm L}^2}{\Delta^2}[2(\hat b_x + \hat b_x^\dagger)\rho(\hat b_x + \hat b_x^\dagger) - (\hat b_x + \hat b_x^\dagger)^2\rho - \rho(\hat b_x + \hat b_x^\dagger)^2]. \quad (57)$$

(Note that we also assume that $\mathcal{E}_{\rm L} \gg \eta_x g_0[\langle \hat a^\dagger \hat a\rangle]^{1/2}$.)

From inspection of the plots of transmission fidelity versus time (for the *overdamped* regime), we can estimate the timescale for state transfer as $\sim 4/\Gamma$. Hence, in order to be able to neglect the effects of spontaneous emission on the transfer process, we require that

$$\frac{\Gamma}{4} = \frac{\eta_x^2 g_0^2 \mathcal{E}_{\rm L}^2}{4\kappa\Delta^2} \gg \eta_x^2\frac{\gamma}{10}\frac{\mathcal{E}_{\rm L}^2}{\Delta^2} \qquad \text{or} \qquad \frac{5g_0^2}{2\kappa\gamma} \gg 1. \quad (58)$$

This, not surprisingly, corresponds to the regime of strong coupling in cavity QED [38].

The dipole coupling strength is given by $g_0 = [3c\lambda^2\gamma/(8\pi V_{\rm m})]^{1/2}$, where λ is the wavelength of the atomic transition and $V_{\rm m} = (\pi/4)w_0^2 l$ is the cavity mode volume, with w_0 the cavity mode waist and l the mirror separation. The cavity field decay rate can be expressed in terms of the mirror separation and the cavity finesse $\mathcal{F}$ as $\kappa = \pi c/(2\mathcal{F}l)$. Using these expressions for g_0 and κ, the condition in (58) can be rewritten in the form

$$\frac{15}{2}\frac{\lambda^2}{\pi^3}\frac{\mathcal{F}}{w_0^2} \gg 1. \quad (59)$$

So, of course, one would like to have small cavity modes and high-finesse mirrors.

The trap itself must also meet rather stringent requirements; in particular, the Lamb–Dicke parameter must satisfy $\eta_j \ll 1$ ($j = x, y, z$) and the trap frequency along the x-axis must satisfy $\nu_x \gg \kappa$. Let us now consider a specific example from the ion-trapping community: the trapped ion species $^9Be^+$. Recent experiments with this particular ion (see, for example, [1, 2]) have been performed with harmonic oscillation frequencies along the principal axes of the trap $\nu_j/2\pi \simeq$ 11–30 MHz, corresponding to Lamb–Dicke parameters $\eta_j \simeq 0.14$–0.086 (with respect to the $^2S_{1/2} \leftrightarrow {}^2P_{1/2}$ transition at wavelength $\lambda = 313$ nm; the linewidth for this transition is $\gamma/2\pi = 19.4$ MHz).

A further practical consideration is the requirement that the spacing between the mirrors be large enough to accommodate the ion-trap electrodes and external laser fields. A reasonable minimum separation might be $l = 100\ \mu$m, but we shall make a somewhat more conservative choice of $l = 250\ \mu$m. With a cavity finesse $\mathcal{F} = 300\,000$†, one then obtains $\kappa/2\pi = 1.0$ MHz. Assuming, say, that $\eta_x = 0.1$, then $\nu_x/2\pi = 22$ MHz and $\nu_x/\kappa = 22$. If the radius of curvature of the mirrors is taken to be 5 cm, then the cavity waist takes the value $w_0 = 15.8\ \mu$m (which yields $g_0/2\pi = 14.9$ MHz) and $15\lambda^2\mathcal{F}/(2\pi^3 w_0^2) = 28 \gg 1$.

Finally, given these choices of parameters, a numerical estimate for the rate $\Gamma = \Omega^2/\kappa$ at which the state transfer occurs in the overdamped regime would be $\Gamma/2\pi \simeq$ 20–200 kHz, and even larger with suitable laser pulse shapes in the underdamped regime. This estimate establishes a

† A finesse of 300 000 corresponds to combined mirror losses of ∼21 ppm. In practice, these losses can be divided into two contributions: mirror transmission (T), which facilitates input and output to the cavity field, and scattering and absorption (A). Clearly, we desire that $T \gg A$ in order for the input/output channel to dominate. Further, to realize an essentially one-sided cavity, as assumed throughout our work, we require the transmission of one mirror to be much larger than that of the second. Mirror transmission and scatter and absorption losses of the order of 1 ppm have been reported by Rempe *et al* [39] at wavelengths near 850 nm. However, achieving such values at wavelengths of 300–400 nm is possibly very demanding of current mirror technology. Note, though, that favourable parameters for our schemes can still be attained with smaller values of the finesse (e.g. 150 000).

timescale for the required stability of the driving laser fields (remember that the phases of the two laser fields are assumed to be equal for the duration of the state transfer process) and of the cavity and trap set-ups. Note that the timescales for motional decoherence and heating observed in recent trapped ion experiments (with $^9Be^+$) are of the order of milliseconds and further improvement seems possible [12].

So, it would seem that, with quite reasonable choices of experimental parameters, a suitable operating regime for the state transfer scheme is feasible. Note that favourable parameters should also be achievable with trapped-ion species other than $^9Be^+$; for example, $^{24}Mg^+$ or $^{40}Ca^+$. Alternatively, recent developments with microscopic magnetic traps [40, 41] suggest that suitably large trap frequencies and confinement in the Lamb–Dicke regime may also be possible with neutral atoms, such as Li and K.

To conclude, in this paper we have described a means of usefully combining several emerging candidate technologies for the implementation of quantum communication and computing, i.e., trapped atoms, cavity QED and propagating (nonclassical) light fields. The schemes outlined above allow, in principle, for the transfer of quantum states and entanglement between light fields and motional degrees of freedom of trapped atoms and for high-fidelity transmission of quantum states between spatially distant sites.

Acknowledgments

We gratefully acknowledge the contributions of Professor S Braunstein, whose insight was crucial in initiating this work. ASP thanks A Doherty, C Hood, Q Turchette, S van Enk, L You and P Zoller for helpful discussions and the ITP in Santa Barbara for its hospitality, where part of this work was carried out, supported in part by the NSF under grant no PHY94-07194. ASP also thanks the Quantum Optics Group at Caltech for its hospitality and acknowledges support from the Marsden Fund of the Royal Society of New Zealand. HJK is supported by the National Science Foundation, by DARPA via the QUIC Institute which is administered by ARO, and by the Office of Naval Research.

Appendix. Cascaded cavities correlation functions

Using equation (25), the equations of motion for the mean values of the two cavity field amplitudes are straightforwardly derived as

$$\langle \dot{\tilde{a}}_1 \rangle = -\kappa \langle \tilde{a}_1 \rangle, \tag{A.1}$$

$$\langle \dot{\tilde{a}}_2 \rangle = -\kappa \langle \tilde{a}_2 \rangle - 2\kappa \langle \tilde{a}_1 \rangle, \tag{A.2}$$

for which the solutions are (for $t \geqslant 0$)

$$\langle \tilde{a}_1(t) \rangle = \mathrm{e}^{-\kappa t} \langle \tilde{a}_1(0) \rangle, \tag{A.3}$$

$$\langle \tilde{a}_2(t) \rangle = \mathrm{e}^{-\kappa t} \langle \tilde{a}_2(0) \rangle - 2\kappa t \mathrm{e}^{-\kappa t} \langle \tilde{a}_1(0) \rangle. \tag{A.4}$$

These solutions are of the general form

$$\langle A_i(t) \rangle = \sum_j f_{ij}(t) \langle A_j(0) \rangle, \tag{A.5}$$

and the quantum regression theorem [24, 25] states that two-time correlation functions follow as

$$\langle A_i(t) A_k(0) \rangle = \sum_j f_{ij}(t) \langle A_j(0) A_k(0) \rangle. \tag{A.6}$$

In steady state, the only nonzero equal-time correlations for our system are

$$\langle \tilde{a}_1 \tilde{a}_1^\dagger \rangle_{\mathrm{ss}} = \langle \tilde{a}_2 \tilde{a}_2^\dagger \rangle_{\mathrm{ss}} = 1, \tag{A.7}$$

which lead to the two-time correlation functions given in (27) and (28).

References

[1] Meekhof D M *et al* 1996 *Phys. Rev. Lett.* **76** 1796
[2] Monroe C *et al* 1996 *Science* **272** 1131
[3] Leibfried D *et al* 1996 *Phys. Rev. Lett.* **77** 4281
[4] Cirac J I *et al* 1996 *Adv. At. Mol. Opt. Phys.* **37** 237 and references therein
[5] Deutsch I H and Jessen P S 1998 *Phys. Rev.* A **57** 1972
[6] Cirac J I and Zoller P 1995 *Phys. Rev. Lett.* **74** 4091
[7] Monroe C *et al* 1995 *Phys. Rev. Lett.* **75** 4714
[8] King B E *et al* 1998 *Phys. Rev. Lett.* **81** 1525
[9] Turchette Q A *et al* 1998 *Phys. Rev. Lett.* **81** 3631
[10] Hughes R J *et al* 1996 *Phys. Rev. Lett.* **77** 3240
[11] Steane A 1997 *Appl. Phys.* B **64** 623
[12] Wineland D J *et al* 1998 *J. Res. NBS* **103** 259
[13] Zeng H and Lin F 1994 *Phys. Rev.* A **50** R3589
[14] Buzek V *et al* 1997 *Phys. Rev.* A **56** 2352
[15] Harrison F E *et al* 1997 *Phys. Rev.* A **55** 4412
[16] Steinbach J, Twamley J and Knight P L 1997 *Phys. Rev.* A **56** 4815
[17] Heinzen D J and Wineland D J 1990 *Phys. Rev.* A **42** 2977
[18] Vogel K and Risken H 1989 *Phys. Rev.* A **40** 2847
[19] Smithey D T *et al* 1993 *Phys. Rev. Lett.* **70** 1244
[20] See also Cirac J I, Lewenstein M and Zoller P 1995 *Phys. Rev.* A **51** 1650
[21] Blatt R 1999 Private communication
[22] See, for example, Kimble H J 1992 *Fundamental Systems in Quantum Optics Proc. Les Houches Session LIII, (1990)* ed J Dalibard *et al* (New York: Elsevier)
[23] Turchette Q A *et al* 1998 *Phys. Rev.* A **58** 4056
[24] See, for example, Gardiner C W 1991 *Quantum Noise* (Berlin: Springer)
[25] See, for example, Walls D F and Milburn G J 1994 *Quantum Optics* (Berlin: Springer)
[26] Gardiner C W 1993 *Phys. Rev. Lett.* **70** 2269
[27] Carmichael H J 1993 *Phys. Rev. Lett.* **70** 2273
[28] Gardiner C W and Parkins A S 1994 *Phys. Rev.* A **50** 1792
Kochan P and Carmichael H J 1994 *Phys. Rev.* A **50** 1700
[29] Boschi D *et al* 1998 *Phys. Rev. Lett.* **80** 1121
[30] Bouwmeester D *et al* 1997 *Nature* **390** 575
[31] Furusawa A *et al* 1998 *Science* **282** 706
[32] Cirac J I *et al* 1997 *Phys. Rev. Lett.* **78** 3221
[33] van Enk S J, Cirac J I and Zoller P 1997 *Phys. Rev. Lett.* **78** 4293
[34] Pellizzari T 1997 *Phys. Rev. Lett.* **79** 5242
[35] van Enk S J *et al* 1999 *Phys. Rev.* A **59** 2659
(van Enk S J *et al* 1998 *Preprint* quant-ph/9805003)
[36] See, for example, Zoller P and Gardiner C W 1997 *Quantum Fluctuations Proc. Les Houches (Session LXIII 1995)* ed S Reynaud *et al* (New York: Elsevier)
[37] See, for example, Cirac J I *et al* 1992 *Phys. Rev.* A **46** 2668
D'Helon C and Milburn G J 1995 *Phys. Rev.* A **52** 4755
[38] Kimble H J 1994 *Cavity Quantum Electrodynamics* ed P Berman (Boston: Academic) p 203
[39] Rempe G *et al* 1992 *Opt. Lett.* **17** 363
[40] Weinstein J D and Libbrecht K G 1995 *Phys. Rev.* A **52** 4004
[41] Vuletic V *et al* 1998 *Phys. Rev. Lett.* **80** 1634